Free Shear flow Coherent Structures

Single point statistics such as $\overline{u}$, $\overline{uv}$, etc. provide limited information describing the actual large scale structure of turbulent flows. 2-point correlation show that the velocity is apparently correlated over distances up to the width of the flow, but here again do not provide an explanation of the instantaneous flow structures.

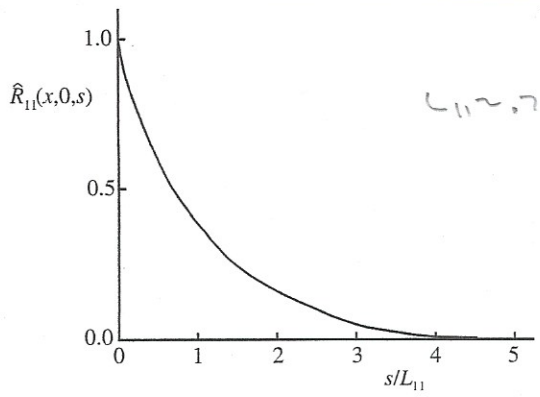

$L_{11} \sim .7 r_{1/2}$

Fig. 5.13. The longitudinal autocorrelation of the axial velocity in the self-similar round jet. From Wygnanski and Fiedler (1969).

Coherent structures: large scale structures "eddies" identified using flow visualization (smoke, dye or hydrogen bubble tracers) and/or one or two-point statistics including conditional sampling. Historically based EFD, but more recently using DNS.

"energetic"

Those large scale anisotropic structures overlay the small scale isotropic turbulence

Structures often similar those observed during transition of associated flow instabilities.

Mixing Layer

Schlieren Photograph

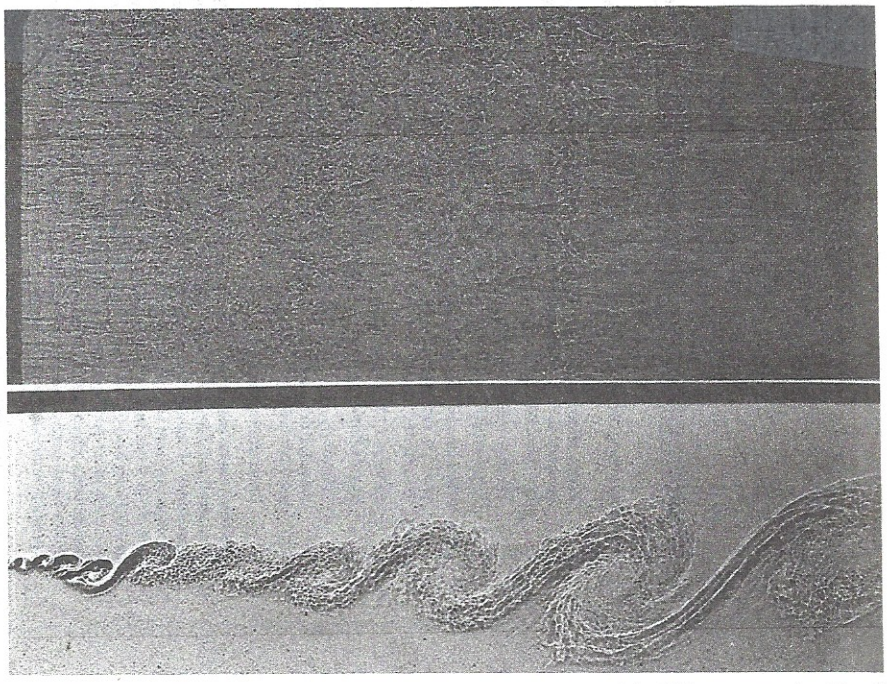

Figure 26.28 Growth of a free-shear layer between streams with different speeds. The lower portion of the photo is a side view; a plan view is reflected in a mirror in the upper portion. Large coherent eddies continue to grow for all downstream distances. Reprinted with permission from Brown and Roshko (1974).

vortices / eddies / rollers

Large scale spanwise that grow at decrease in number as flow develops down stream, similar to KH instability. A roller can merge with adjacent roller in pairing process or can be torn apart & absorbed by adjacent roller. Eddies grow by entrainment or by vortex pairing

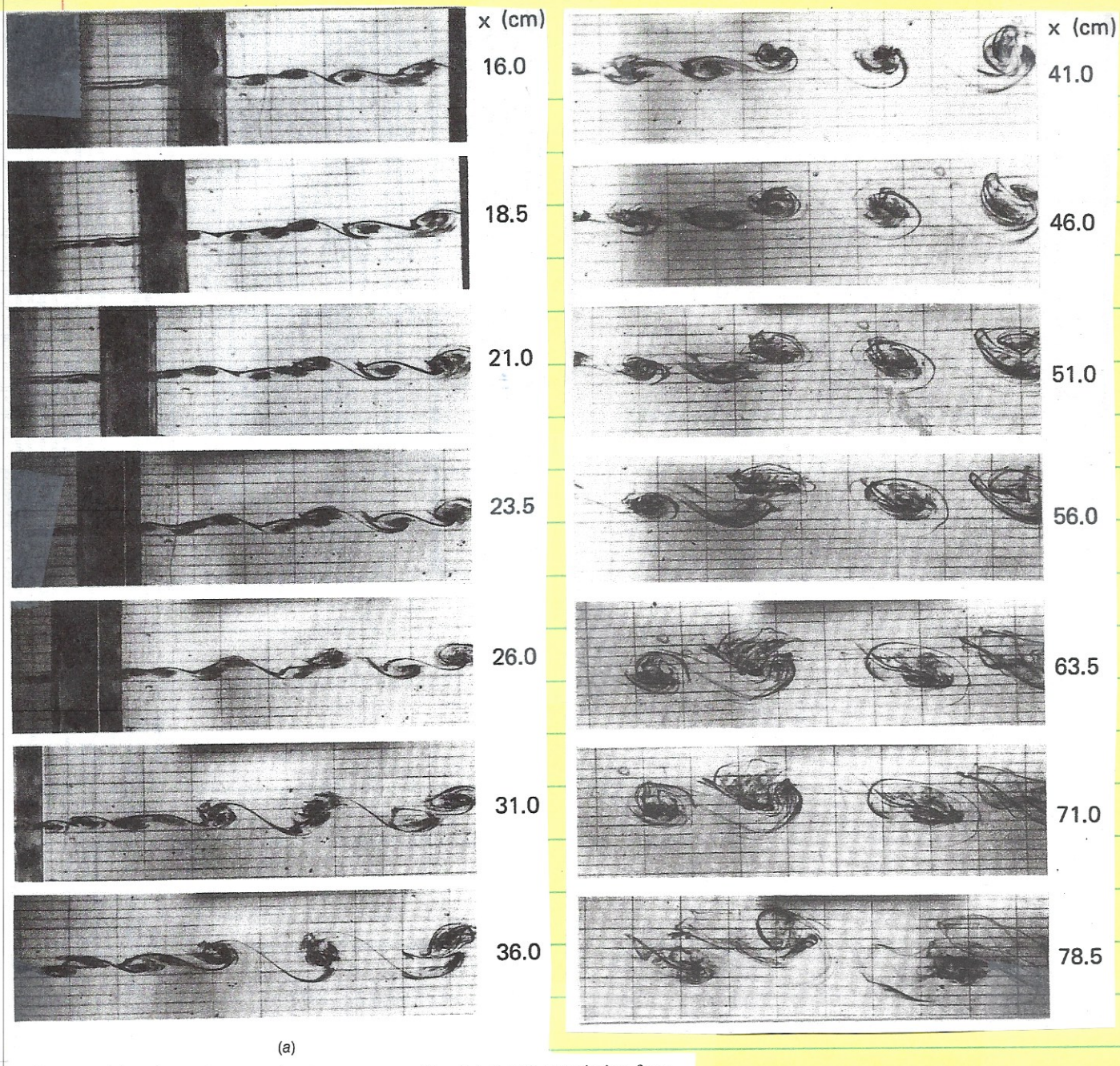

(a)

Figure 26.29 Vortex pairing shown in a step-by-step sequence. Reprinted with permission from Winant and Browand (1974), Cambridge University Press. Numbers indicate downstream distance of the camera.

Observe: small scale eddies within large eddies
evidence of secondary longitudinal instability

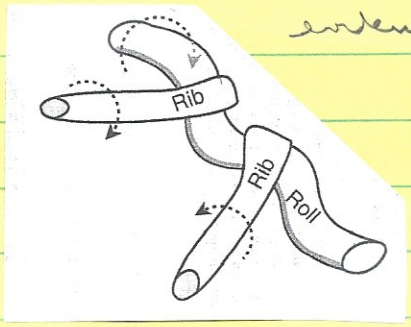

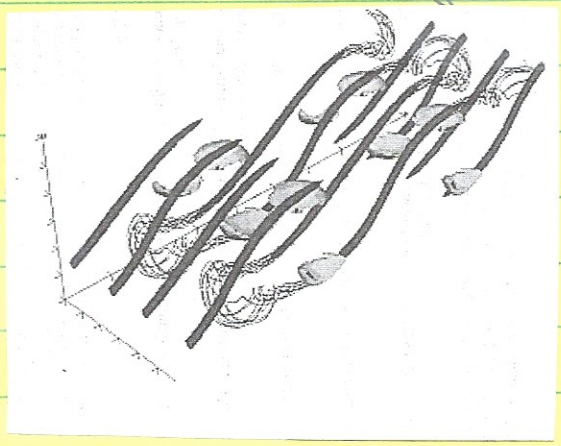

Figure 5.34 *Left: schematic of ribs wrapping around and distorting rolls. Right: ribs in a transitional mixing layer, as seen via contours of* $\sqrt{\omega_x^2 + \omega_y^2}$*; reproduced from Moser & Rogers (1991), with permission.*

Roll vortices stretch connecting fluid "braids" and wx vortices develop on the braids. Important for mixing on smaller scales than rollers. Shear layer grows via entrainment of & completes mixing process.

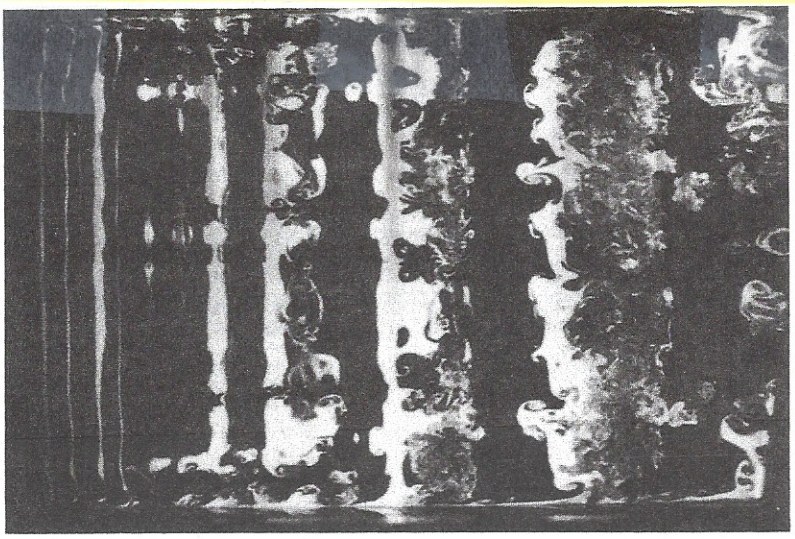

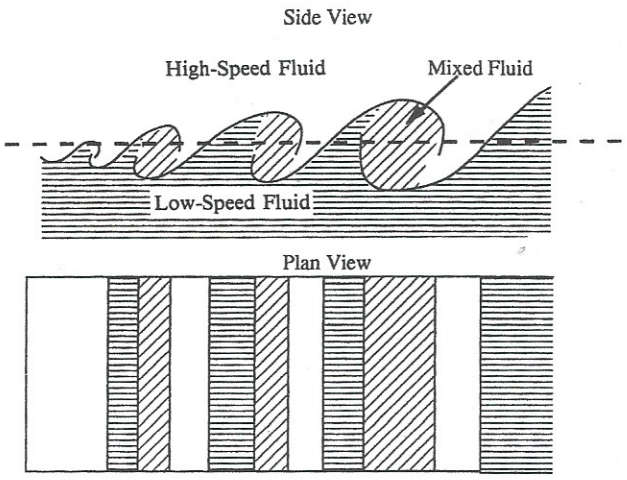

Figure 26.30 Flow visualization of a mixing layer in a plan view. Lower low-speed fluid is marked with fluorescent dye and illuminated by a sheet of light, as indicated by the dashed line in the pictorial side view. The pictorial plan view indicates regions of fluid corresponding to the photograph. The regions on the right show counterrotating vortices (mushroom shapes) on the braids between vortices. Reprinted with permission from Bernal and Roshko (1986), Cambridge University Press.

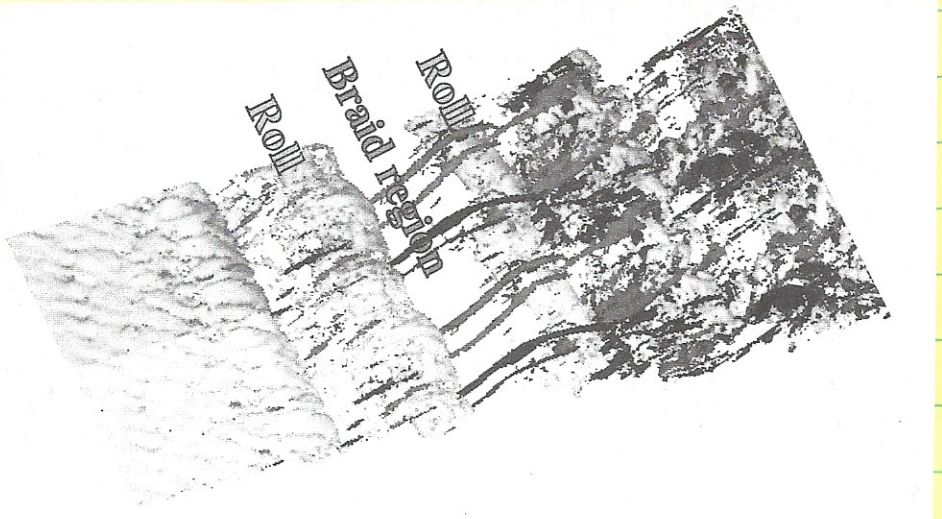

Figure 5.35 *Rolls and Ribs in a transitional mixing layer: contours of streamwise vorticity, ω_x. The grey and black streamwise contours, seen between the rolls, are the edges of positive and negative vortices of the braid region. Figure courtesy of P. Comte and P. Bégou (Comte et al., 1998).*

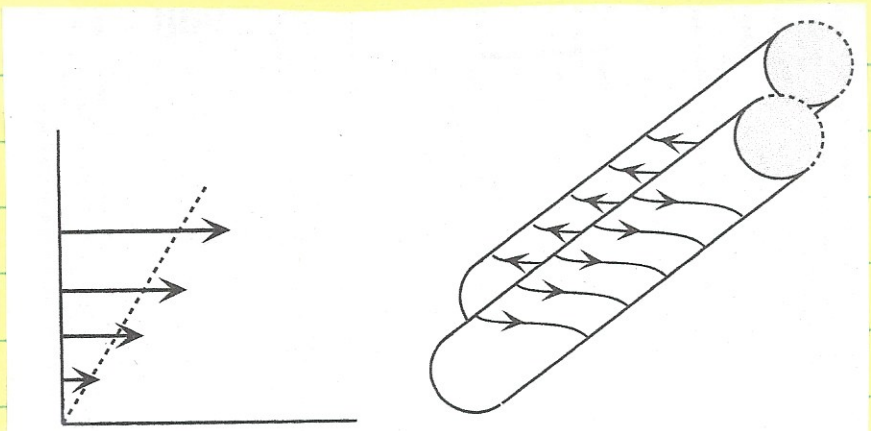

Figure 5.36 *Double rollers in free-shear flows, after Townsend (1976).*

Two-point correlations show double rollers in planar free shear flows, which align at 40° to the shear.

natural mixing layer
little evidence rollers

periodic forcing
induces vortex pairing
& increased
growth of mixing
layer

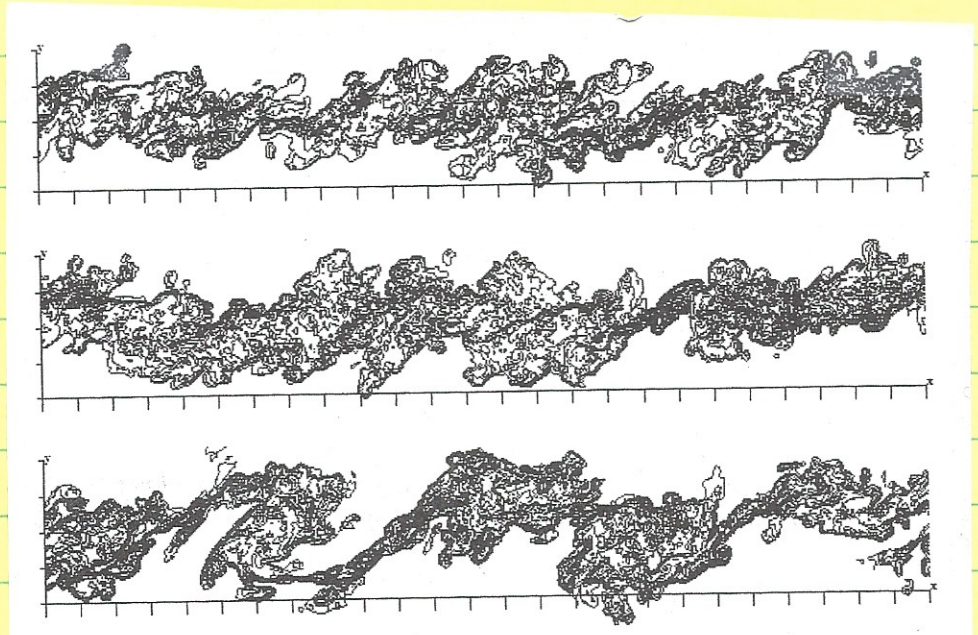

Figure 5.37 *From Rogers & Moser (1994); reproduced with permission. Contours of a passive tracer delineate mixing layer eddies. Top: a natural mixing layer; middle: a mixing layer subject to moderate, periodic forcing; lower: a mixing layer with strong forcing.*

Jets

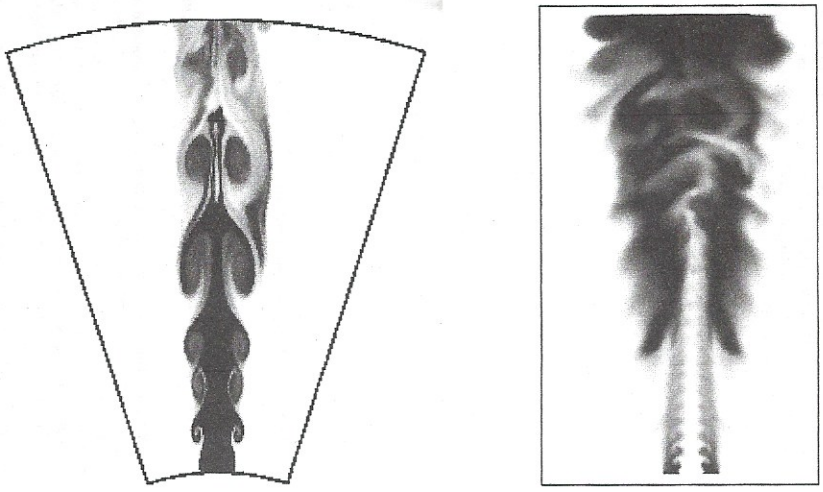

Figure 5.33 *Jets undergoing transition to turbulence, visualized via a scalar concentration field. From numerical simulations by Steiner & Busche (1998) and Danaila & Boersma (1998).*

Large ring shaped vortices become corrugated / irregular inducing vortex pairing at breakup

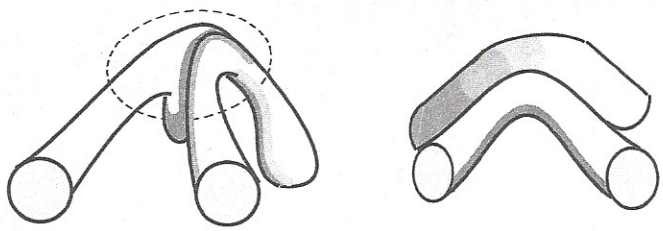

The two original tubes merge in the circled region, then fission to create two new tubes at a different orientation, as at right.

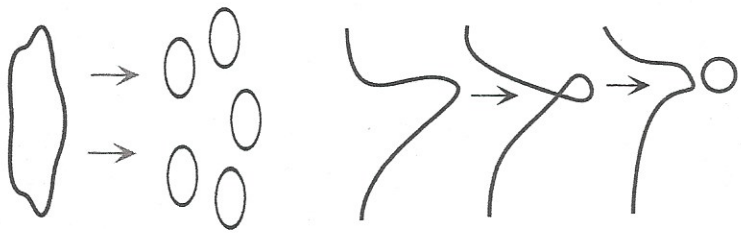

At left, circular vortices in a jet break up to form smaller eddies via the cut and connect process. At right, hairpin vortices can pinch off a ring.

Figure 5.38 *Reorganization of vortices: cut and reconnection of vortex tubes, following Hussain (1978)*

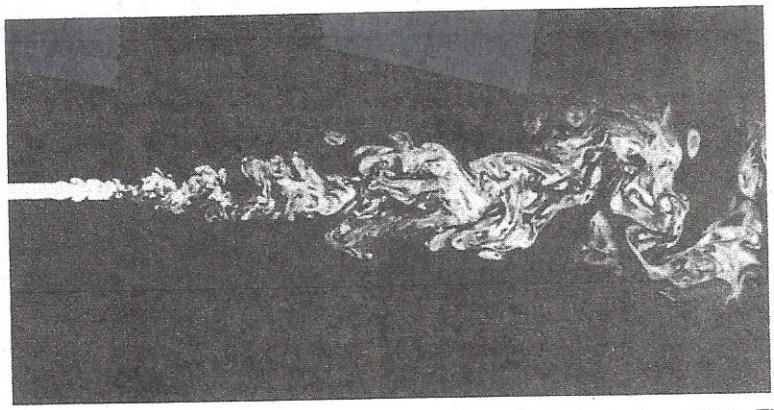

Figure 26.6 Turbulent water jet visualized in a plane on the axis at $\mathrm{Re} = 2300$. The picture resolution exceeds the Kolmogorov scale in the right half. Also note the spiral structure. Reprinted with permission from Dimotakis et al. (1983). Copyright 1983, American Institute of Physics.

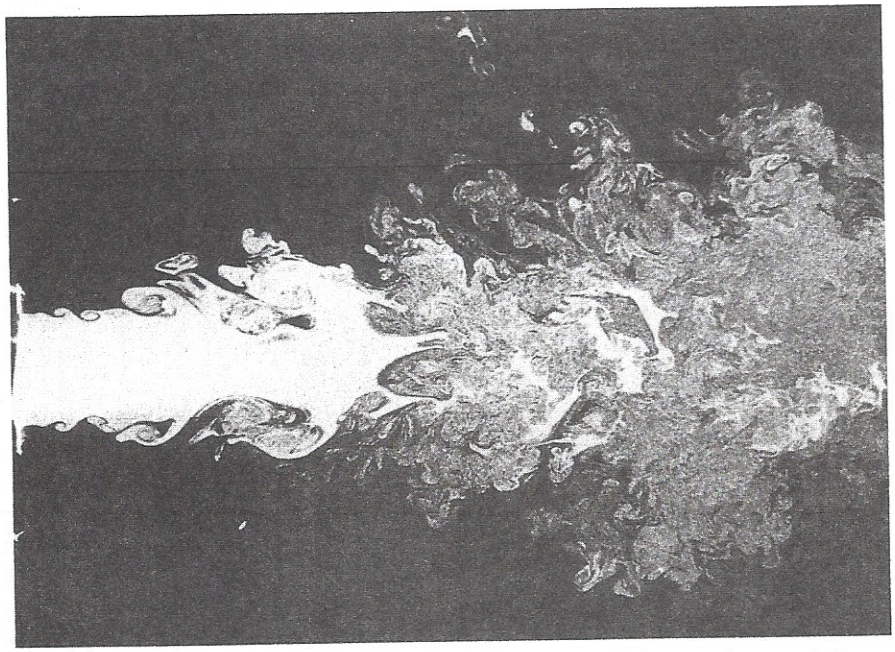

Figure 26.7 Turbulent air jet at a higher Reynolds number (11,000) shows an increase in fine–scale structure. Courtesy of J. L. Balint, M. Ayrault, and J. P. Schon, École Centrale de Lyon, France. Work described by Balint et al. (1982).

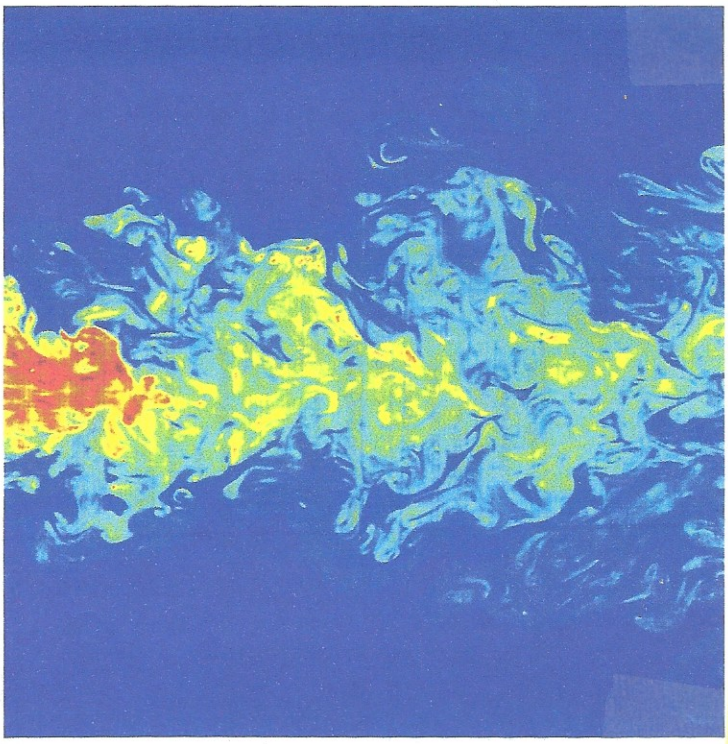

Plate 6 A turbulent jet made visible by laser-induced fluorescence. Note the convoluted outer edge of the jet. [Picture by C. Fukushima and J. Westerweel, University of Delft. Courtesy of efluids.com.]

Bifurcating Blooming Jet

Helical perturbation
axi/helical f = 2
jet bifurcates into
two distinct branches
f = 1.7 – 3.5 vortex
rings sent all
directions = blooming
jet Re = 5000, f = 2.3

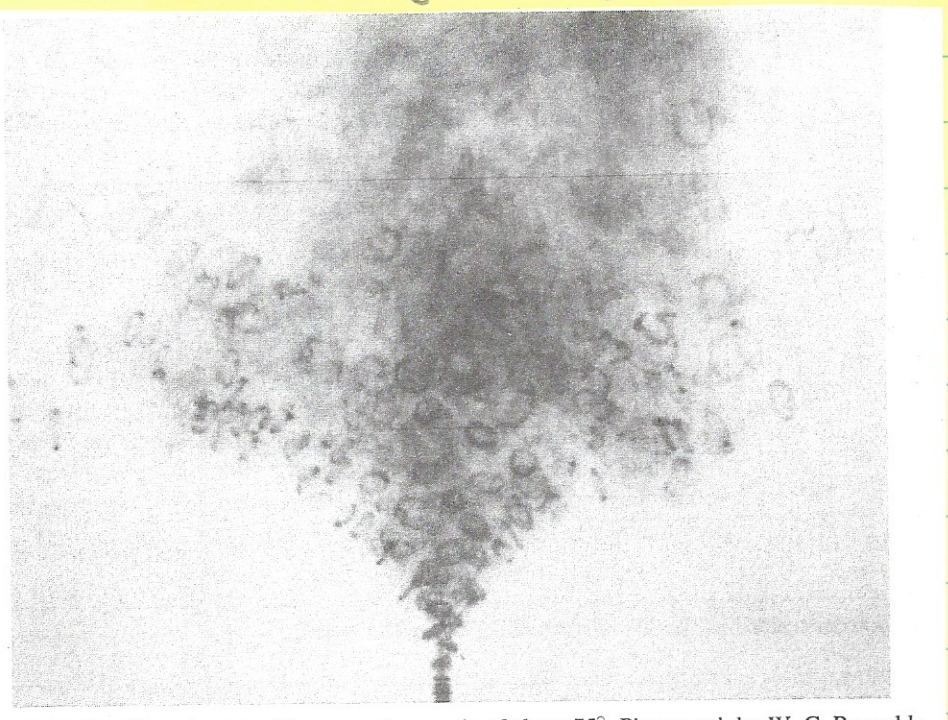

Figure 26.31 Blooming jet with a spreading angle of about 75°. Photograph by W. C. Reynolds, Stanford University.

Wakes

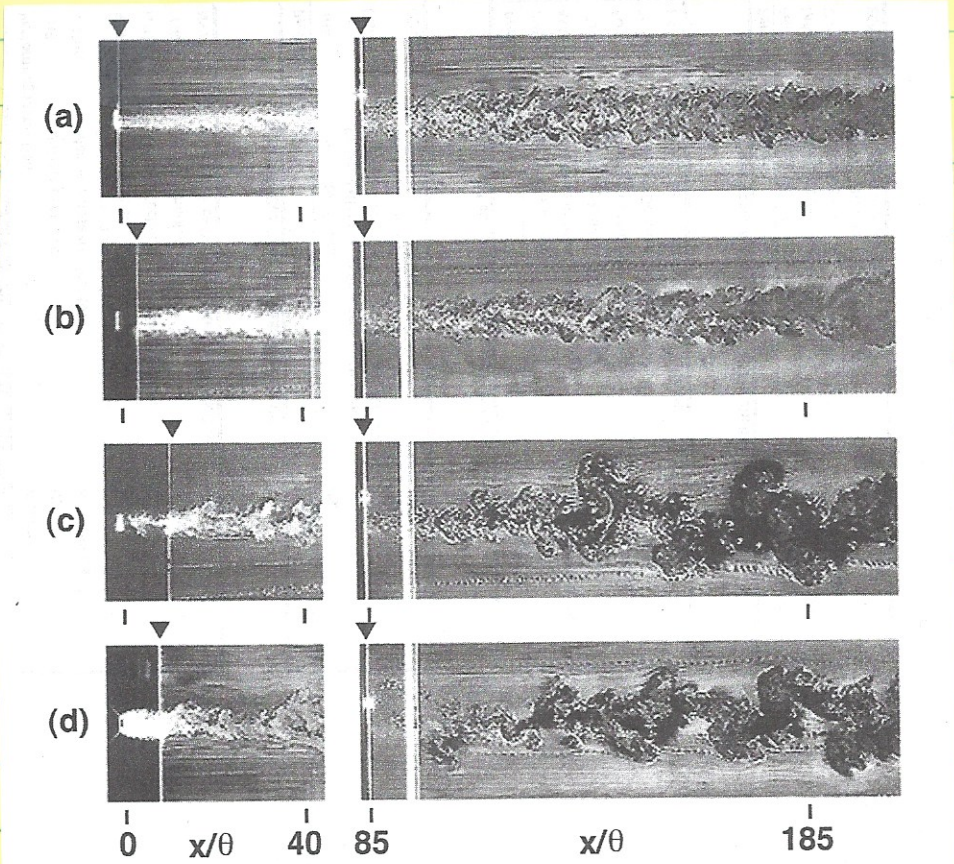

Fig. 5.52. A visualization of statistically axisymmetric wakes: (a) 50%-blockage screen, (b) 60%, (c) 85%, (d) 100% (i.e., a disk). The momentum thickness of the wake is θ; smoke wires are located at $x/\theta = 10$ and $x/\theta = 85$. (From Cannon *et al.* (1993) with permission of Springer-Verlag.)

Large scale motion with dominant f
ie $S = f_L/U = f$ (geometry, body) of
related flow instabilities such as Karmon
shedding of KH (shear layer) of responsible
differences rate of spreading

Table 5.3. *The spreading parameter and turbulence intensity for axisymmetric wakes behind various bodies*

Body	Spreading parameter S	Turbulence intensity on centerline $\langle u^2\rangle_0^{1/2}/U_s$	Investigation
49% blockage-screen	0.064	0.3	Cannon and Champagne (1991)
6:1 spheroid	0.11	0.3	Chevray (1968)
84% blockage-screen	0.34	0.75	Cannon and Champagne (1991)
Sphere	0.51	0.84	Uberoi and Freymuth (1970)
Disk	0.71	1.1	Cannon and Champagne (1991)
Disk	0.8	0.94	Carmody (1964)

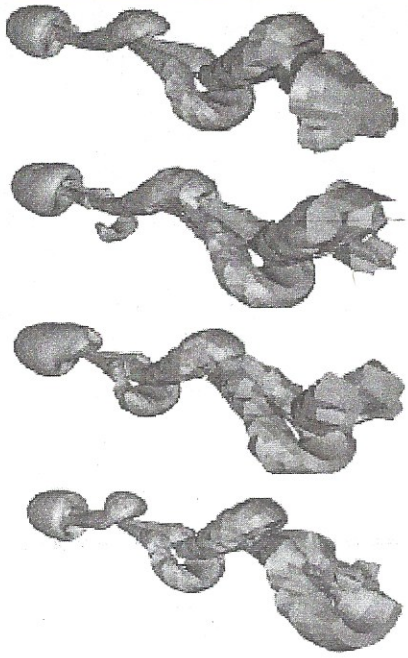

Figure 5.39 *Vortical structures downstream of a sphere. The surfaces enclose regions where rate of rotation is greater than rate of strain. The loops rotate direction to create a helical signature. From Johnson & Patel (1999), reproduced with permission.*

Wake sphere different circular jet. Sphere wake shows helical structure. Loops of vortices are shed creating helical structures